

N62558-02-M-5607

SHOCK STUDIES OF CERAMICS
(Visiting Scientist Dr N S Brar)

Final Technical Report
by

Dr W G Proud, Professor J E Field
August 2002

United States Army

EUROPEAN RESEARCH OFFICE OF THE US ARMY

London, England

CONTRACT NUMBER N62558-02-M-5607

PCS
University of Cambridge
Department of Physics
Cavendish Laboratory
Madingley Road
Cambridge
CB3 0HE
UK

DISTRIBUTION STATEMENT A
Approved for Public Release
Distribution Unlimited

20020801 193

REPORT DOCUMENTATION PAGE

Form Approved
OMB No. 0704-0188

Public reporting burden for this collection of information is estimated to average 1 hour per response, including the time for reviewing instructions, searching existing data sources, gathering and maintaining the data needed, and completing and reviewing this collection of information. Send comments regarding this burden estimate or any other aspect of this collection of information, including suggestions for reducing this burden to Washington Headquarters Services, Directorate for Information Operations and Reports, 1216 Jefferson Davis Highway, Suite 1204, Arlington, VA 22202-4302, and to the Office of Management and Budget, Paperwork Reduction Project (0704-0188), Washington, DC 20503

1. AGENCY USE ONLY (Leave blank)		2. REPORT DATE 31 August 2002	3. REPORT TYPE AND DATES COVERED May - August 2002	
4. TITLE AND SUBTITLE Shock Studies of Ceramics Visiting Scientist Dr N S Brar			5. FUNDING NUMBERS N62558-02-M-5607	
6. AUTHOR(S) Dr W G Proud Professor J E Field				
7. PERFORMING ORGANIZATION NAME(S) AND ADDRESS(ES) University of Cambridge Department of Physics, Cavendish Laboratory, Madingley Road, Cambridge CB3 0HE, UK			8. PERFORMING ORGANIZATION REPORT NUMBER RG 35823	
9. SPONSORING / MONITORING AGENCY NAME(S) AND ADDRESS(ES) European Research Office of the US Army 223 Old Marylebone Road London NW1 5TH, UK			10. SPONSORING / MONITORING AGENCY REPORT NUMBER	
11. SUPPLEMENTARY NOTES				
12a. DISTRIBUTION / AVAILABILITY STATEMENT Distribution unlimited			12b. DISTRIBUTION CODE	
13. ABSTRACT (Maximum 200 Words) The report covers the visit of Dr N S Brar of the University of Dayton, USA to the Cavendish Laboratory. The project involved an exchange of ideas in the area of shock physics and the design, sample preparation and testing of various materials in the plate-impact facility. The report describes the plate impact facility and the techniques used. A phenomena of particular interest is that of failure front propagation in brittle materials. This is failure by compression and shear rather than tension. It is an established phenomena for glasses, but its occurrence in ceramics needs further study. The study visit was valuable in developing collaboration between the University of Dayton and the Cavendish.				
14. SUBJECT TERMS Shock Plate Impact Ceramics			15. NUMBER OF PAGES	
			16. PRICE CODE ¹²	
17. SECURITY CLASSIFICATION OF REPORT Unclassified	18. SECURITY CLASSIFICATION OF THIS PAGE Unclassified	19. SECURITY CLASSIFICATION OF ABSTRACT Unclassified	20. LIMITATION OF ABSTRACT SAR	

SHOCK STUDIES OF CERAMICS

Visiting Scientist Dr N S Brar

1. Background

This covered a 3 month period visit, starting April 2002, by Dr N S Brar of the University of Dayton, USA.

The area of research involved shock studies of materials using the technique of plate-impact. This is a technique of interest to both ARL and Cambridge. The aims were (i) to study failure front propagation in glasses and ceramics, (ii) to build up useful collaboration between the two groups.

2. The plate-impact method and the facilities at the Cavendish Laboratory

Impulsive loading conditions need to be considered in many industries including structural strength of vehicles during crash situations, lightweight body armour for personnel and military vehicles, aero-engines and space-craft. As such situations arise under diverse conditions, there is a need to be take account of these in the materials selection and design process. To do this effectively, it is necessary to understand the material response to high stress loading at high loading rates.

In plate impact experiments, the impacting plate is fired at a target. If there is good alignment, a 1-d pulse of chosen pressure and duration can be produced. The pressure generated depends on the Hugoniot properties of the plate and target materials and the impact velocity. The duration is controlled by the to and fro transit time of the shock in the plate. The 1-d pulse is maintained until release waves from the plate and target boundaries reach the target axis. This effectively defines the "window" for accessing data.

All the experiments reported here were carried out using the single stage gas gun in the Cavendish Laboratory (figure 1).



Figure 1: Plate impact facility at Cavendish Laboratory

The projectile consists of a flyer plate attached to a polycarbonate sabot. It is placed in the barrel and held against the breech block by a vacuum. Two "O" rings on the sabot, block the exits of the two reservoirs. This arrangement is known as a "wrap-around" breech. The reservoirs are filled with propellant gas using pressurised cylinders and compressors operating up to 350 bar. When using helium as a propelling gas, velocities of up to 1.2 km/s can be achieved. As noted above, by altering the impact speed and the material of the flyer plate, the impact stress can be varied.

The gun is fired by the rotation of a solenoid which breaks the vacuum behind the projectile causing it to move forward, clearing the reservoir exits. The high pressure gas then accelerates the sabot and flyer plate down the barrel. The barrel is 5 m long, has a 50 mm bore accurate to $\pm 25 \mu\text{m}$ along its length.

Projectile velocity is measured to an accuracy of $\pm 0.5\%$ by means of four pairs of pins which are positioned at accurately known distances before the target. As the conductive flyer passes a pair of these pins, it completes a circuit giving a shorting signal which is recorded on an oscilloscope. Graphite pins, diameter 0.3 mm, are used to measure velocities below 600 m/s and brass pins for higher velocities.

Stress levels are measured in the sample with Manganin gauges or using velocity interferometry (VISAR; velocity interferometry system for any reflector).

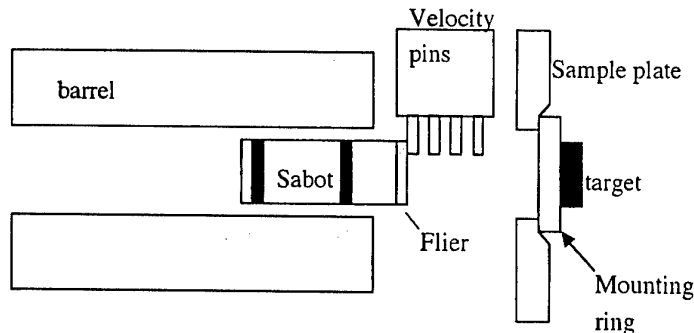


Figure 2: Experimental set-up for plate impact experiment (not to scale).

For a 1-d loading impact, the sample, mounting, mounting ring, sample plate and flyer plate need to be flat *and* aligned. At the end of production, the projectile is held in a lathe and the flyer plate is faced to be perpendicular to the rotation axis of the sabot. The sample plate is aligned to an accuracy of $0.1 \mu\text{m}$ by use of a dial gauge and a plug inserted in the end of the barrel for each experiment.

The mounting ring is machined flat and parallel to better than $10 \mu\text{m}$ over its 14 cm diameter. The central hole of the ring is diameter 6 cm which allows the projectile to pass through after the impact. The ring is lightly pressed into place on the sample plate, figure 2. The target is fixed to the ring using metal filled epoxy, which has good adhesion and minimal expansion on setting; care is taken not to get adhesive between the target and mounting ring. At impact, the sabot is partially in the barrel so ensuring that there is no yaw due to gravity acting on the projectile.

The particle velocity-time history of a specularly reflecting surface during an impact can be determined using VISAR. It is important that the surface is not polished to an optical finish because such a finish is unlikely to be preserved at high stress. This technique was developed by Barker et al. in the late 60's and early 70's.

The reflected laser light is captured and split into two beams, one of which is passed through a glass cylinder known as an "etalon". Because the refractive index of glass is higher than that of air, the light in this beam is slowed down and delayed with respect to the other beam which passes through air. If the target is stationary, the interference pattern will not change with time when the two beams are recombined. For an accelerating target, however, the reflected beam will be doppler shifted, and due to this change in frequency, there is a beat frequency when the two beams are recombined. Changes in velocity can be measured by recording this interference. The time delay is dependent on the "etalon" length, so it is possible to adjust the system to ensure that an appropriate amount of acceleration per beat (fringe) is obtained. VISAR effectively measures the rear surface particle velocity from which a shock pressure versus time trace can be obtained. Rise times of $\sim 2\text{ns}$ can be followed.

Various gauge types are also used. These involve cutting up the target, mounting the gauge and re-assembly of the target. Gauges can be used to measure longitudinal or lateral stresses. The longitudinal gauge gives "in target" pressure information, the subtraction of the lateral stress from the longitudinal stress gives twice the shear strength.

3. Failure Fronts

3.1 Glasses

In contrast to work on ceramics, the interpretation of the significance of the HEL in glasses is different. Brar *et al.* (1991) have shown that the spall strength of the material behind the shock front remains finite even when shocked to above the HEL. However, they found that a failure front ran behind the shock and that behind this the spall strength fell dramatically as observed earlier by Kanel and his co-workers (Kanel *et al.* 1992). In order to investigate this phenomenon and to clarify the meaning of the failure front Cambridge has conducted a series of plate impact tests with simultaneous high-speed photography to observe the fronts (Bourne *et al.* 1994). The gauge experiments have utilised the lateral gauge technique described above. In each of the two experiments for which traces are shown in figure 3 the impactor was a 6mm thick copper plate. The sample was float glass of density 2490 kg m^{-3} and longitudinal sound speed $5.92\text{ mm }\mu\text{s}^{-1}$. The lower traces (solid lines) represent longitudinal and transverse gauge records for an impactor velocity of 610 m s^{-1} . The longitudinal record for an impact at 750 m s^{-1} is also presented (dotted line). The longitudinal gauges were placed on the rear surface of the glass block in PMMA as described above and the shock reflects from the PMMA/glass interface back into the shocked material as a release. The rise shows a ramping, viscous response. After the initial rise, the stress in both the lateral and longitudinal traces drop slightly. Simultaneous high-speed photography associates this dip with a dark front visible in the pictures. The ratio of the longitudinal to lateral stress is initially *ca.* 3:1 as expected from elasticity theory with a Poisson's ratio of 0.25.

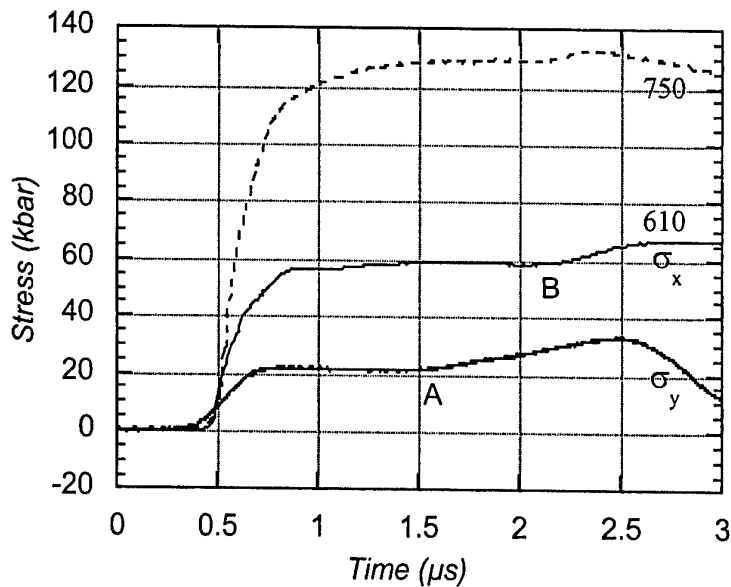


Figure 3. Plate impact experiments on float glass at 610 (solid line) and 750 $m s^{-1}$ (dotted line). The impactor is in each case a 6 mm thick copper plate. The lower two traces represent the longitudinal and transverse gauge measurements for the same experiment. A marks the arrival of the failure front at the transverse gauge. B marks the arrival of a compressive reflection from the failure front at the gauge location. The same feature can be seen on the higher velocity shot.

Point A marks the arrival of a failure front at the lateral location. The convergence of the lateral and longitudinal records from A onwards indicates the reduction in the shear strength across the failure front. The rise in lateral stress at A is not mirrored in a corresponding rise in longitudinal stress. However at point B the longitudinal stress does rise. This is due to the arrival of a compression wave which is a reflection from the failure front of the release from the gauge location. The same feature can be seen on the qualitatively similar high velocity trace coming in at the same time.

By performing a series of experiments with match conditions, it is possible to produce a graph of the initial and final shear strength of the glass targets. The results for several different filled glasses are shown in figure 4. It can be seen that above a certain stress the failure phenomena occurs, the shear strength before the passage of the failure front remains close to that of the elastic line. However, the shear strength after the passage of the shock wave falls dramatically. As the samples are struck with greater velocities this degraded shear strength, after falling to a minimum, then increases with impact. This effect has been seen in granular materials such as cement paste and corresponds to the fragments caused by the failure front become locked together by the increased compressive forces.

A remarkable observation is the similarity of response of many of the glasses, attributed to the presence of the silicon-oxygen network in all these glasses (Brar and Espinosa 1998; Brar 2000).

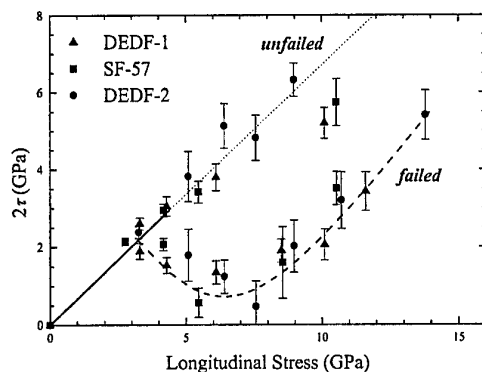


Figure 4. Deviatoric responses of dense glasses tested up to ca. 14 GPa longitudinal stress. From Radford et al. (2001).

An example of the value of high-speed photography can be seen in figure 5, in which the mechanism of failure can be interpreted. The sequence was taken using an Ultramac FS501 with lighting from a xenon flash. Each frame was exposed for 50 ns and the interframe time is displayed at the lower corner of each frame. The flyer impacts onto a float glass target at 250 m s^{-1} from the top of the frame, inducing a dark front S which travels downwards. Along the centre of the frame there is a vertical fiducial line which represents the central impact axis and on which are placed two markers at distances of 15 and 20 mm from the impact face. The field of view of the frame is thus of the order $15 \text{ mm} \times 10 \text{ mm}$. The longitudinal gauge trace obtained for an impact on a similar sample shows the stress wave ramping up to a peak value during a period of roughly 300 ns and thereafter remaining constant behind the shock. The dark areas in the photographs correspond to regions in which the density changes, giving rise to refraction of light out of the shock. Where the density (and thus refractive index) remains constant to the rear of the shock, light is not refracted and enters the lens. Calculating the thickness of the shock from a measurement of the ramp rise time agrees well with the thickness of the dark band in the photographs.

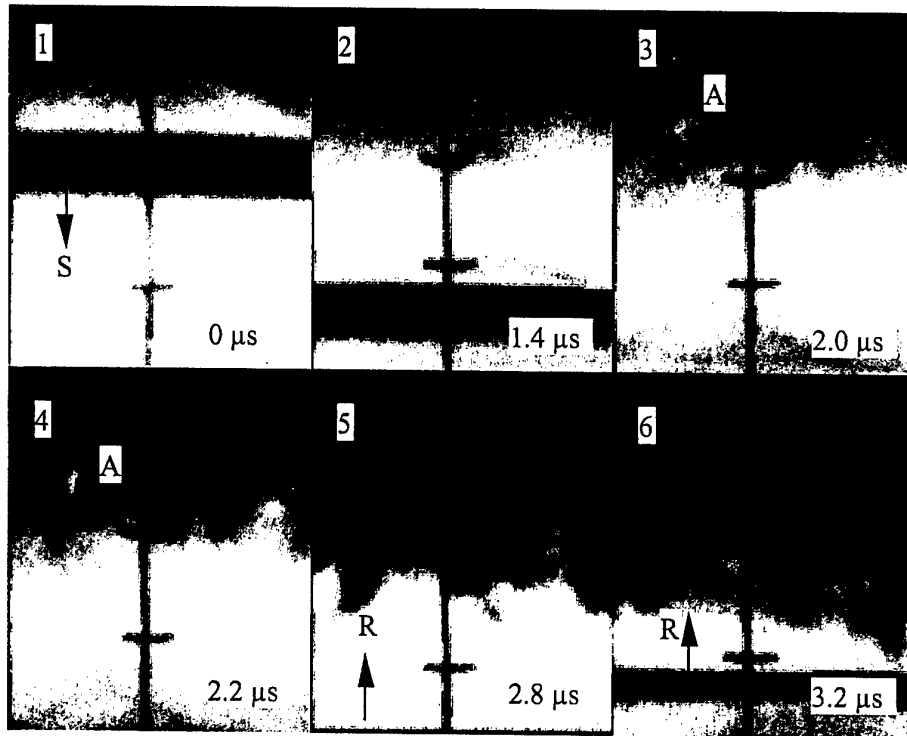


Figure 5. Soda-lime glass impacted from the top at 250 m s^{-1} . A shock S travels down through the frames, leaving in frame 2. The scale markers are 5 mm apart and the first is 15 mm from the impact face. A failure front appears behind in frame 2 and a damage site, A , nucleates and grows in frames 3 and 4. The reflected release R from the free surface enters the frame from below in frames 5 and 6. The exposure time for each frame is 50 ns .

From Bourne et al. (1995).

In frame 2 of the sequence, taken $1.4 \mu\text{s}$ later, a dark irregular front can be seen to the rear of the shock. It has the appearance of a series of bifurcating cracks propagating behind the compression front. Since the depth of field is limited, several cracks can be seen in focus whilst others propagate out of plane and so are out of focus. The distance between the shock and the failure front is about 7 mm . An interesting feature of the failure mechanism can be seen in frames 3 and 4, taken 150 ns apart. A dark point a little to the left-hand side and below the label, A , can be seen forming in frame 3, which grows in frame 4. This is interpreted as the nucleation of failure at a local inhomogeneity within the glass. The failure front can be seen propagating further in frames 5 and 6. More points of nucleation can be seen growing in later frames. The velocity of the failure front as measured from the framing photographs was about 2 km s^{-1} . A reflected release wave, R , propagates from the free rear surface of the target and can be seen in frames 5 and 6. It should be noted that the thickness of the shock wave in the photographs may appear to be slightly thicker than it is in reality due to parallax. The release wave R is thinner than the shock wave S which can be explained by noting that the ramping compression wave upon loading becomes a shock wave upon unloading due to the decreasing moduli with pressure.

In these plate impact experiments, failure is induced by compression and shear **not** tension! The failure front mechanism is still a matter of debate, some current attempts at modelling the system suggest that damage to the material is continuous between the

shock and the failure front. In this scheme the failure front is not a wave in the normal sense rather it is a point at which the damage has increased sufficiently to manifest itself as a black zone where the shear strength degrades. Clearly, a large amount of stored energy is released on failure, which separates the failure surfaces sufficiently for the cracks to be visible despite the large superimposed compressive stresses. Defects appear to act as nucleation sites, but whether these are at an atomic level or at a more macroscopic level has yet to be determined.

The behaviour of glass represents a good illustration of the value of measuring wave profiles in order to deduce damage mechanisms. This research also emphasises the differences between glass compositions (soda-lime, borosilicate and various highly filled lead glasses) which show markedly different behaviours from that described here (Bourne *et al.* 1996).

(b) Ceramics

There is still controversy about the presence of failure fronts in ceramics. Since most ceramics are opaque, high-speed photography (as illustrated in Figure 5) cannot be used. Instead, reliance has to be on gauge traces.

Failure fronts have been found in ceramics under specific situations. For example, when the sample has been cut to add a gauge and the impact is with a "soft" flyer such as copper. The idea is that the copper exploits the interface in the sample and this triggers the failure front.

One way of testing this hypothesis is to use harder flyer materials (steel or tungsten) which are less likely to flow and hence exploit the interface.

Four lateral shots were performed to assess the possibility of the so-called failure front existence in ceramics. Three shots were performed in Syntox CL and one in SiC-B.

Two gauges were placed in each target sample at different thicknesses from the impact site.

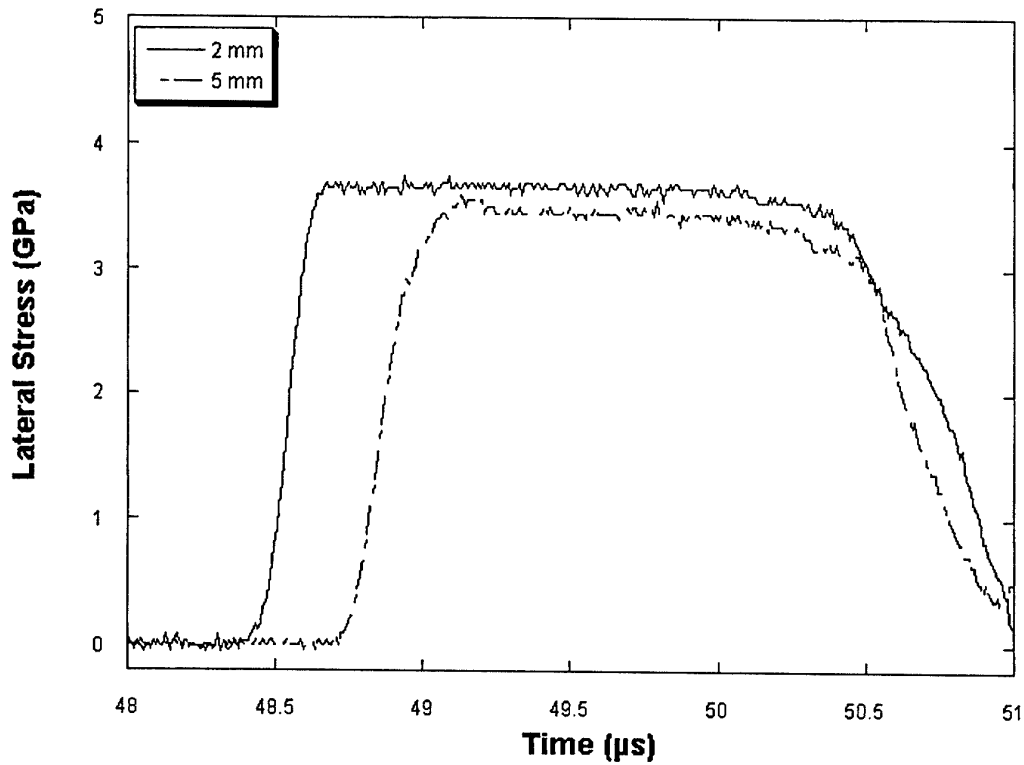


Figure 6: 6.35 mm Steel impacting Syntox CL at 556 m/s. Two gauges, at 2 and 5 mm from impact site. No failure front detected on trace. The difference in height can be attributed to attenuation and dispersion due to first gauge and material nature.

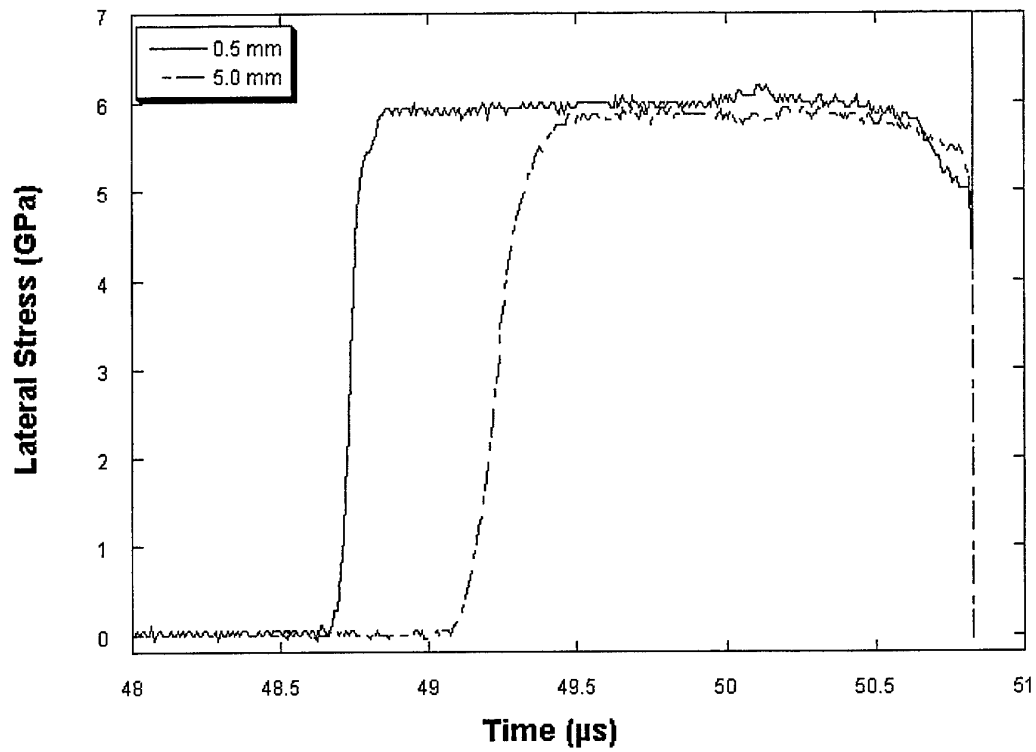


Figure 7: 6.31 mm Steel impacting Syntox CL at 760 m/s. Two gauges, at 0.5 and 5 mm from impact site. No failure front detected from traces.

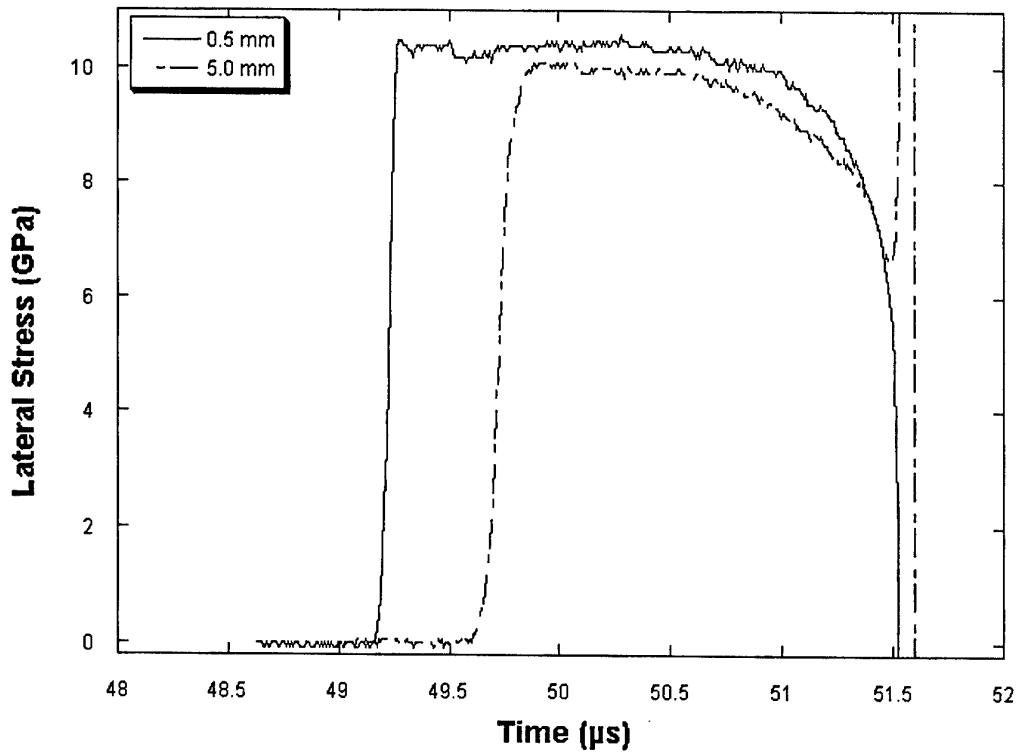


Figure 8: 5.01 mm Tungsten impacting Syntox CL at 807 m/s. Two gauges, at 0.5 and 5 mm from impact site. No failure front detected on trace.

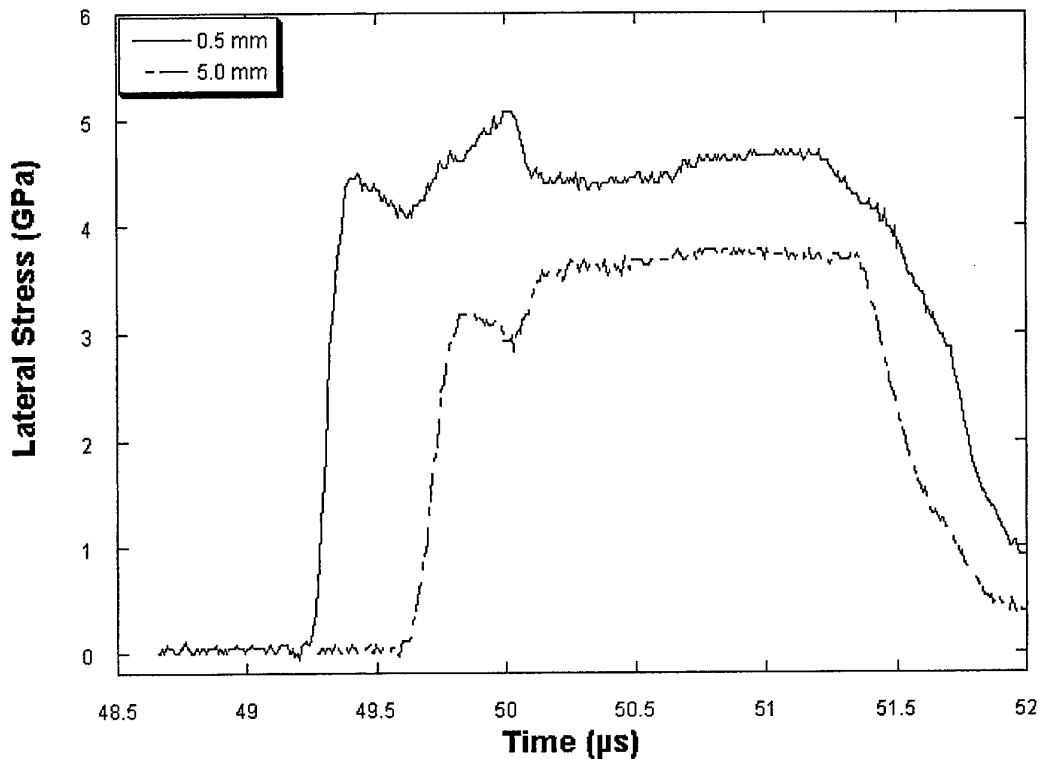


Figure 9: 6.34 mm Steel impacting SiC-B at 807 m/s. Two gauges, at 0.5 and 5 mm from impact site. Failure front detection uncertain.

The tentative conclusion to date is that failure fronts are less likely in ceramics and when they appear it involves a soft flyer exploiting an interface running from the impact face in the direction of loading.

Since failure fronts are failure in compression and shear, it is probably the superior shear strength (hardness) of ceramics which controls this. Note they are 5 to 6 times harder than glasses.

References

Bourne, N.K., Rosenberg, Z. and Ginzburg, A. (1996) The ramping of shock waves in three glasses, *Proc. R. Soc. Lond. A* **452** 1491-1496.

Bourne, N.K., Rosenberg, Z., Mebar, Y., Obara, T. and Field, J.E. (1994) A high-speed photographic study of fracture wave propagation in glasses, *J. Phys. IV France* **4 Colloq. C8 (DYMAT 94)** 635-640.

Bourne, N.K., Rosenberg, Z. and Field, J.E. (1995) High-speed photography of compressive failure waves in glasses, *J. Appl. Phys.* **78** 3736-3739.

Brar, N.S., Rosenberg, Z. and Bless, S.J. (1991) Spall strength and failure waves in glass, *J. Phys. IV France* **1 Colloq. C3 (DYMAT 91)** 639-644.

Brar, N.S. and Espinosa, H.D. (1998) A review of micromechanics of failure waves in silicate glasses, *Chem. Phys. Rep.* **17** 317-342.

Kanel, G.I., Raseorenov, S.V. and Fortov, V.E. (1992) The failure waves and spallations in homogeneous brittle materials, in *Shock Compression of Condensed Matter – 1991*, ed. S.C. Schmidt, R.D. Dick, J.W. Forbes and D.G. Tasker, publ. Amsterdam, Elsevier: pp. 451-454.

Radford, D.D., Proud, W.G. and Field, J.E. (2001) The deviatoric response of three dense glasses under shock loading conditions, to be published in *Proc. 2001 APS Meeting on Shock Compression of Condensed Matter*.

4. Conclusions

The visit period was valuable to both Dr Brar and the Cavendish. Dr Brar gave talks and a colloquium and all members of the group discussed their projects with Dr Brar.

More research will be continued on this joint project and Dr Brar will return to Cambridge during September. This will be funded separately to the present contract.

A Journal paper is being prepared and copies will be sent to the ERO.

There now continues to be regular and useful contact with Dr Brar and other researchers at ARL.